Study on a W-band modified V-shaped microstrip meander-line traveling-wave tube*

Shen Fei(沈 飞), Wei Yan-Yu(魏彦玉)†, Xu Xiong(许 雄),
Yin Hai-Rong(殷海荣), Gong Yu-Bin(宫玉彬), and Wang Wen-Xiang(王文祥)

National Key Laboratory of Science and Technology on Vacuum Electronics, University of Electronic Science and Technology of China, Chengdu 610054, *China*

(Received 10 August 2011; revised manuscript received 8 October 2011)

The study on a miniaturized, low-voltage, wide-bandwidth, high-efficiency modified V-shaped microstrip meander-line slow-wave structure is presented. This structure is evolved from the original U-shaped microstrip meander-line slow-wave structure, combining the advantages of a traditional microstrip and a rectangular helix. In this paper, simulations of the electromagnetic characteristics and the beam-wave interaction of this structure are carried out. Our study shows that when the design voltage and the current of a sheet electron beam are set to be 4700 V and 100 mA, respectively, this miniature millimeter-wave power amplifier is capable of delivering 160-W output power with a corresponding gain of 37.3 dB and a maximum interaction efficiency of 34% at 97 GHz.

Keywords: modified V-shaped microstrip meander-line, millimeter-wave power amplifier, beam-wave interaction, slow-wave structure

PACS: 42.60.Da, 07.57.Hm, 41.20.Jb **DOI:** 10.1088/1674-1056/21/6/064210

1. Introduction

Nowadays, the millimeter-wave spectrum, especially the relatively low atmospheric attenuation in the vicinity of 94 GHz, is one of the most actively used spectrums, with applications such as high-data-rate communications, radar and electronic warfare.[1−3] The millimeter-wave traveling-wave tube (TWT) is a vital part of modern millimeter-wave amplifiers[4−11] due to their combined performances in bandwidth, power capacity, gain variation, and linearity.

In the microwave device community, there is a significant interest in compact and light weight millimeter-wave amplifiers with moderate power and wide bandwidth capabilities. One of the most promising millimeter-wave amplifiers that can satisfy the above requirements, especially at the Ka-band and the Q-band frequencies, is the helix TWT.[12−14] However, as the operating frequency extends to W-band or above, the fabrication of helix circuits is a crucial challenge.[15] The micro-fabrication technique, as a way to solve this problem, is more naturally applicable to two-dimensional (2D) structures.[16] Therefore, as a three-dimensional (3D) structure, the fabrication process of the helix circuit will be rather complicated and difficult. It is essential for us to find a new type of slow-wave structure (SWS) which retains the advantages of helix TWTs but overcomes their fabrication problems.

A novel V-shaped slow-wave transmission line, of the microstrip type, called V-shaped microstrip meander-line SWS, has been proposed for low voltage, wide bandwidth, and moderate power miniature TWTs. It has a periodic structure with a period length of L in the longitudinal propagation direction, and its fabrication is very convenient when utilizing 2D MEMS technology. This V-shaped microstrip meander-line SWS, as a new type of slow-wave structure, is evolved from the original U-shaped microstrip meander-line SWS,[17] combining the advantages of a traditional microstrip and a rectangular helix.[18,19] In order to enhance the output power, this V-shaped microstrip meander-line SWS is improved by using a V-shaped dielectric rod instead of a dielectric substrate.

In this paper, the electromagnetic characteristics of this structure, including the dispersion characteristics, interaction impedance, and transmission characteristics, are investigated by using the CST-MWS.[20] Its beam-wave interaction is also calculated with the

*Project supported by the National Natural Science Foundation of China (Grant No. 60971038) and the Fundamental Research Funds for the Central Universities (Grant No. ZYGX2009Z003).

†Corresponding author. E-mail: yywei@uestc.edu.cn

© 2012 Chinese Physical Society and IOP Publishing Ltd

particle-in-cell (PIC) algorithms in the CST-PS.[21]

2. System description

As shown in Fig. 1, the shielded V-shaped microstrip meander-line SWS is comprised of a partially filled dielectric rectangular waveguide and a novel V-shaped metal strip having specific transverse and longitudinal dimensions. Its modified form, the modified V-shaped microstrip meander-line SWS, consisting of a periodic V-shaped metal strip each having a period length of L and a V-shaped dielectric rod, is depicted in Fig. 2. Here, the dielectric material filling the rectangular waveguide is no longer a dielectric substrate, but a periodic V-shaped dielectric rod instead. It is the significant difference between the original structure and the modified structure, wherein a and h are the width and the height of the rectangular waveguide; $h_{\rm d}$ is the thickness of the dielectric substrate and it is also the height of the dielectric rod.

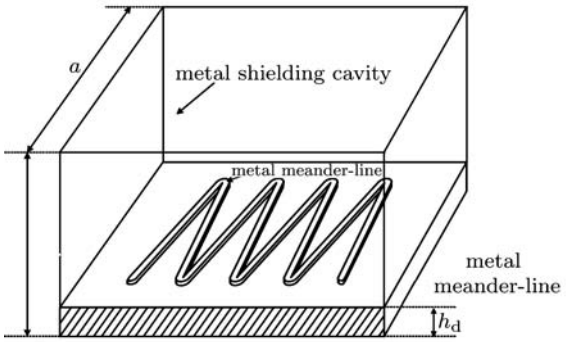


Fig. 1. Model of the shielded V-shaped microstrip meander-line SWS.

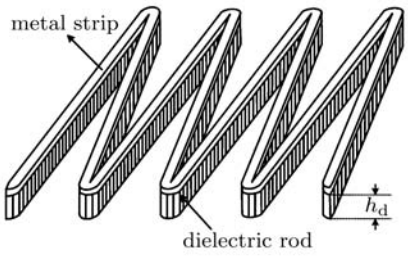


Fig. 2. Model of the modified V-shaped microstrip meander-line SWS.

Figure 3 shows dimensional parameters of the V-shaped metal strip, wherein b is the transverse width of the metal strip; p is the length of a single pitch; θ is the bending-angle of the V-shaped metal meander-line; w and t are the width and the thickness of the metal strip, respectively.

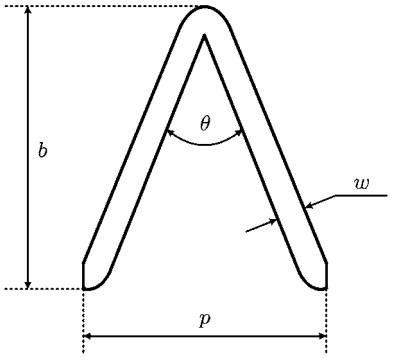


Fig. 3. Dimensional parameters of the V-shaped metal strip.

3. Electromagnetic properties

In this section, the electromagnetic properties including dispersion characteristics and interaction impedance are presented by utilizing the eigen mode solver of the CST-MWS under the periodic boundary condition. Subsequently, the transmission characteristics will be calculated by the transient solver in CST Microwave Studio. In this paper, our study focuses on the W-band, and the longitudinal central axial position of the sheet electron beam is 0.05 mm over the periodic V-shaped metal strip. In Table 1, the optimized structural parameter values of the modified V-shaped microstrip meander-line SWS are presented.

Table 1. Optimized structural parameters.

Parameter	Value
a/nm	1.056
b/nm	0.528
p/nm	0.112
w/nm	0.024
t/nm	0.005
h/nm	0.85
h_d/nm	0.05
θ/(°)	7.6

In order to highlight the advantages of the modified V-shaped microstrip meander-line SWS, the comparisons of dispersion characteristic and interaction impedance between the original structure and its modified structure are carried out. Here, all the dimensional parameters of the two SWSs are set to be equal.

From Fig. 4, we can obtain that the cold bandwidth of the modified structure ranges from 11.6 GHz to 140 GHz, and that of the original structure is in a range from 9.3 GHz to 113 GHz. Obviously, the cold-bandwidth of the modified structure is much broader than that of the original structure. Furthermore, the

interaction impedance of the modified structure is higher than that of the original structure as well.

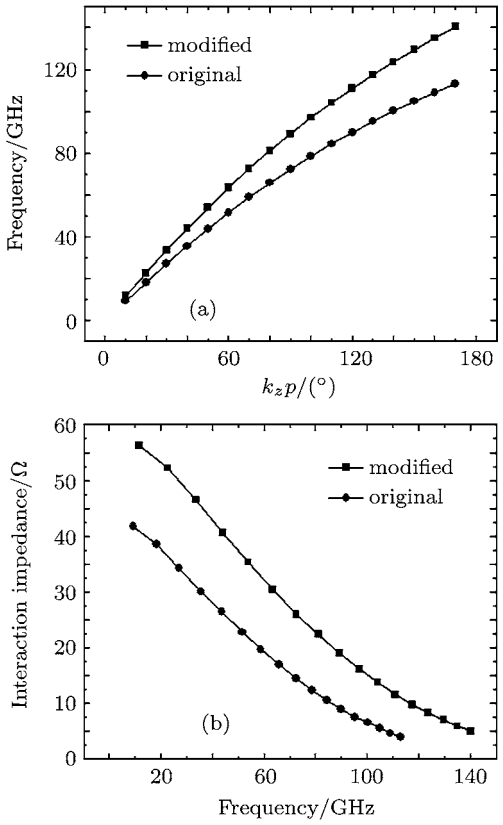


Fig. 4. (a) Dispersion characteristics and (b) interaction impedance comparison between two microstrip meander-line slow-wave circuits.

In Figs. 5 and 6, the influences of some important dimensional parameters of the modified V-shaped microstrip meander-line SWS on dispersion characteristic and interaction impedance are investigated. As the thickness of the dielectric rod or the metal strip increases, the dispersion property becomes worse, whereas the interaction impedance becomes larger in the operating frequency band we required, ranging from 80 GHz to 100 GHz. Since these two parameters can easily affect the dispersion property and the interaction impedance of this modified structure, we should choose proper sizes to satisfy our requirements.

In this part, the loss of the modified V-shaped microstrip meander-line slow-wave circuit, besides the energy input or output coupling structure, is calculated. In our simulations, the metal conductivity is 2.25×10^7 S/m,[22] the relative permittivity of the dielectric rod is 4.[23]

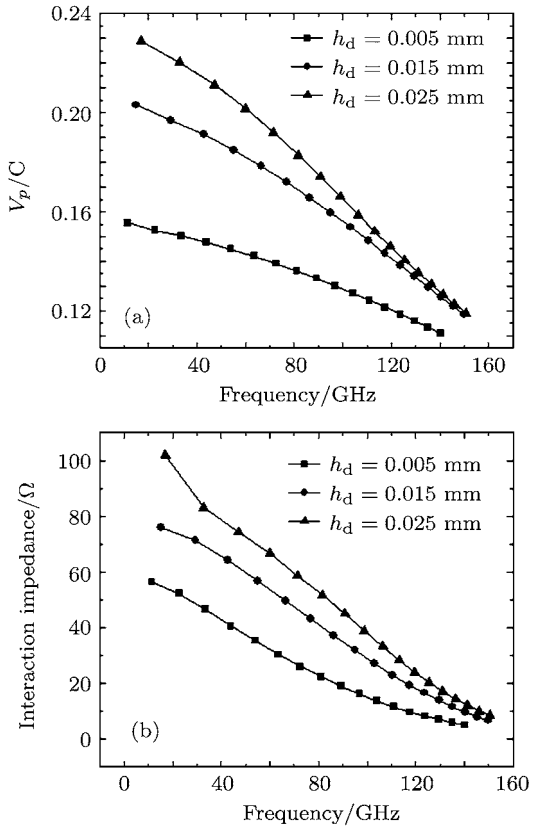


Fig. 5. (a) Dispersion properties and (b) interaction impedances versus thickness of the dielectric rod.

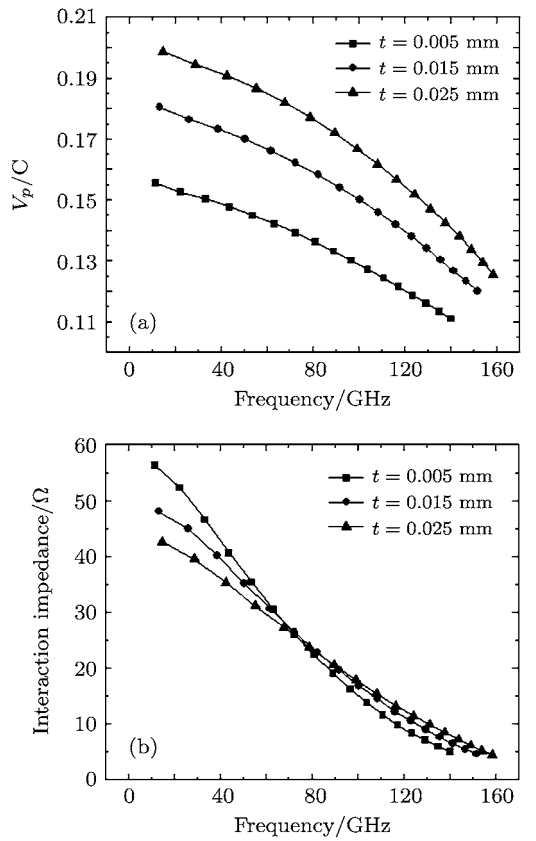


Fig. 6. (a) Dispersion properties and (b) interaction impedances versus thickness of the metal strip.

As is well known, the total transmission loss $\alpha_{\rm t}$ is composed of conductor loss $\alpha_{\rm c}$ and dielectric loss $\alpha_{\rm d}$. In order to calculate $\alpha_{\rm c}$ and $\alpha_{\rm d}$, we assume the boron nitride to be loss free and the V-shaped metal strip to be a perfect electric conductor (PEC), then

$$\begin{cases} \alpha_{\rm t} = \alpha_{\rm c} + \alpha_{\rm d}, \quad \text{copper } (\sigma = 2.25 \times 10^7), \quad \text{boron nitride } (\varepsilon_{\rm r} = 4, \quad \tan\delta = 0.00025), \\ \alpha_{\rm t\ case\ 1} = \alpha_{\rm c} + 0, \quad \text{copper } (\sigma = 2.25 \times 10^7), \quad \text{boron nitride } (\varepsilon_{\rm r} = 4, \quad \tan\delta = 0), \\ \alpha_{\rm t\ case\ 2} = 0 + \alpha_{\rm d}, \quad \text{PEC } (\sigma = \infty), \quad \text{boron nitride } (\varepsilon_{\rm r} = 4, \quad \tan\delta = 0.00025), \end{cases} \tag{1}$$

where $\alpha_{\rm t}$, $\alpha_{\rm t\ case\ 1}$, and $\alpha_{\rm t\ case\ 2}$ can be obtained by using the transient solver in the CST-MWS. Then, $\alpha_{\rm c}$ and $\alpha_{\rm d}$ can be generated from the solutions to Eq. (1), respectively. From Figs. 7 and 8, we can find that the reflection loss S_{11} is below –20 dB ranging from 80 GHz to 105 GHz. Meanwhile, the total loss $\alpha_{\rm t}$ is too small (less than 0.095 dB/mm), and the conductor loss $\alpha_{\rm c}$ is much larger than the dielectric loss $\alpha_{\rm d}$ as shown in Fig. 8.

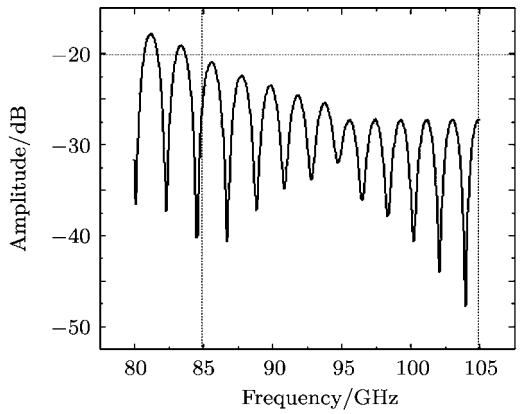


Fig. 7. Reflection loss S_{11} of the modified V-shaped microstrip meander-line SWS.

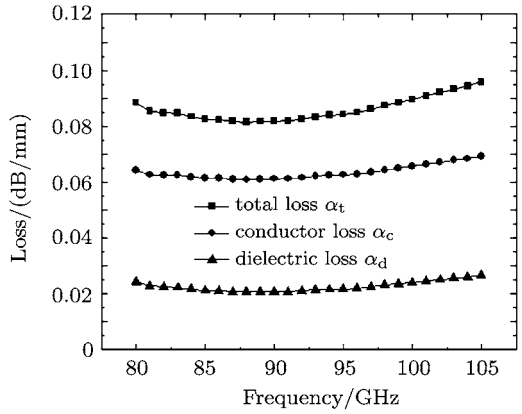


Fig. 8. Loss of the modified V-shaped microstrip meander-line SWS.

Figure 9 shows the longitudinal electric field distribution of the fundamental mode. From Fig. 9, we see that the longitudinal electric field covers the entire width of the slow-wave circuit. Therefore, the width of the sheet electron beam can be designed to be equal to the circuit transverse width for pursuing the maximum output power.

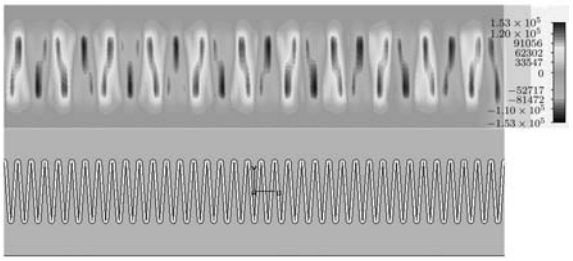


Fig. 9. Patterns of axial electric field.

4. Beam-wave interaction simulations

In this section, large-signal analyses are carried out via the PIC solver in CST-PS based on the optimized parameters given above. The whole slow-wave circuit has a length of 21 mm. In order to obtain a large enough gain and suppress the backward wave oscillation, the whole interaction circuit is divided into four sections, and the section lengths are 25, 25, 25, and 61 pitches, respectively. Two adjacent sections are separated by an attenuator with a length of 15 pitches, and the relative permittivity and the dielectric loss tangent of the material are 11.5 and 0.3.[24] The amplitude of the focusing magnetic field is set to be 1.4 T.[25] Finally, the optimized operating parameters for our modified V-shaped microstrip meander-line TWT are shown in Table 2.

Figures 10 and 11 show the particle velocity modulation along the axial direction and the electron bunching phenomenon, respectively. As shown in Fig. 10, we can see that most of the electrons are decelerated and a small number of electrons are accelerated. Consequently, most of the kinetic energy of the sheet electron beam is transferred to the high frequency electromagnetic field. Then, the excitation signal power will be amplified. Figure 11 shows

the electron bunching phenomenon around the end of the circuit. The electrons are periodically accelerated and retarded along the longitudinal direction, which demonstrates a beam-wave energy exchange process.

Table 2. Operating parameters for a 97-GHz TWT.

Parameter	Value
Beam voltage	4700 V
Beam current	0.1 A
Beam cross sectional area	0.528 mm×0.05 mm
Center frequency	97 GHz
Input power	30 mW
Saturated output power	160 W
Saturated efficiency	34%
Saturated gain	37.3 dB

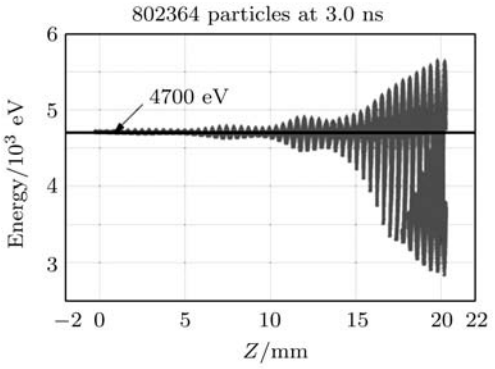


Fig. 10. Beam energy versus longitudinal distance.

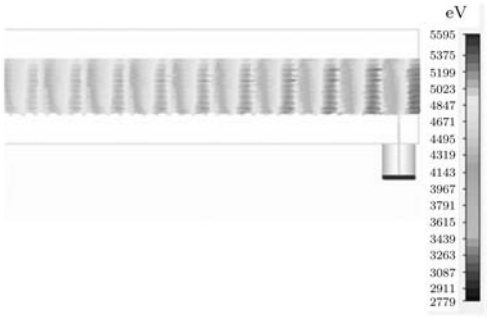


Fig. 11. Electron bunching phenomenon at 97 GHz.

Figure 12 depicts the time-domain features of the input signal and the output signal. From the figure, a steady-state output signal is seen after a transient time of about 2 ns. That is to say, energy exchange between the sheet electron beam and the drive signal is already stable. Meanwhile, the reflection signal is small enough to be ignored.

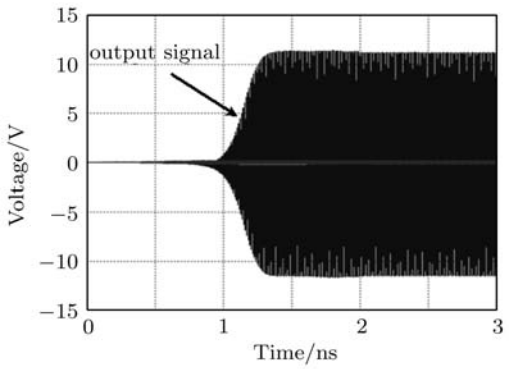


Fig. 12. Input signal and the output signal.

Figure 13 shows the frequency spectrum of the output signal obtained from the Fourier transformation. As can be seen, there is only a single frequency at 97 GHz in the frequency spectrum. That is to say, this modified V-shaped microstrip meander-line SWS is almost free from oscillation.

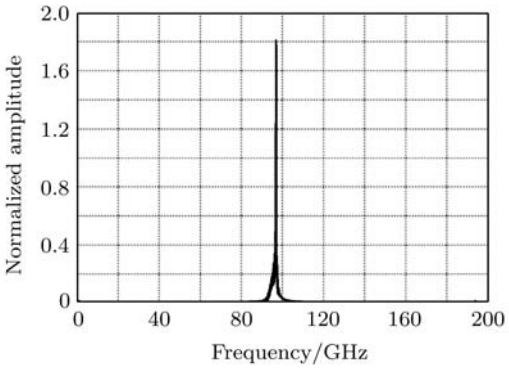


Fig. 13. Spectrum of the output signal.

The frequency sweep is performed in order to examine the instantaneous bandwidth at a constant input power. Figure 14 gives the plots for saturated output power and the corresponding gain versus drive frequency. As can be seen, this modified V-shaped microstrip meander-line TWT can deliver output powers of more than 67 W at least covering the frequency range of 80 GHz–100 GHz. Moreover, the peak output power is 160 W at 97 GHz, corresponding to the gain and electron efficiency of 37.3 dB and 34%, respectively.

Figure 15 shows the output power as a function of input power and the corresponding gain. We can see that the gain decreases as the input power increases. And as the input power increases to 30 mW, the output power becomes saturated.

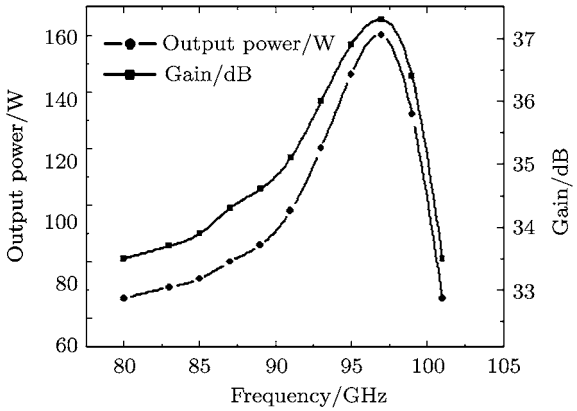


Fig. 14. Output power and gain versus frequency.

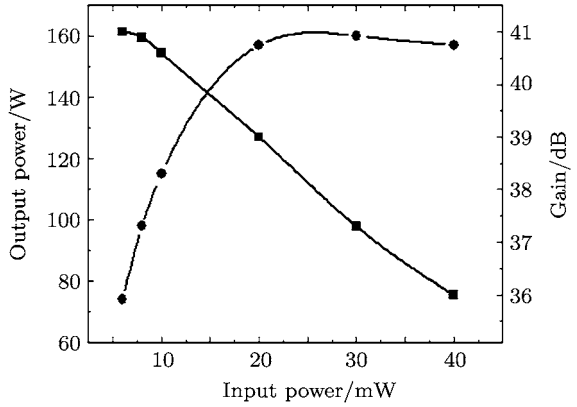


Fig. 15. The output power and gain versus the input power.

5. Conclusion

This modified V-shaped microstrip meander-line TWT inherits the advantages of both traditional microstrips and a rectangular helices. It is a compact, low voltage, broad bandwidth, high efficiency, and high power millimeter-wave power amplifier. As a microstrip structure, its fabrication process is rather simple and convenient by utilizing 2D MEMS technology. Furthermore, this kind of slow-wave circuit is well compatible with the solid-state circuit, abd therefore it is maybe an attractive choice for W-band MMPM. Therefore, this modified V-shaped microstrip meander-line TWT can be considered to be a promising millimeter power amplifier for the future.

References

[1] Fen J J, Hu Y F, Cai J, Wu X P and Tang Y 2010 *Vacuum Electronics* **52** 27 (in Chinese)

[2] Zhong K, Yao J Q, Xu D G, Zhang H Y and Wang P 2011 *Acta Phys. Sin.* **60** 034210 (in Chinese)

[3] Guo Z, Fan F, Bai J J, Niu C and Chang S J 2011 *Acta Phys. Sin.* **60** 074218 (in Chinese)

[4] Fen J J, Cai J, Hu Y F, Wu X P, Ma S Y and Qu B 2009 *Proc. Institute of Chinese Electronics Conf. on Microwave Tubes* September 12–15, 2009, Yichang, China p. 5 (in Chinese)

[5] He J, Wei Y Y, Gong Y B and Wang W X 2010 *Acta Phys. Sin.* **59** 2843 (in Chinese)

[6] He J, Wei Y Y, Gong Y B and Wang W X 2010 *Acta Phys. Sin.* **59** 6659 (in Chinese)

[7] He J, Wei Y Y, Gong Y B and Wang W X 2011 *Chin. Phys.* B **20** 054102

[8] Gao X, Yang Z Q, Cao W P and Jiang Y N 2011 *Chin. Phys.* B **20** 030703

[9] Jiang B, Zhang Y J, Zhou W J, Chen W, Liu A J and Zheng W H 2011 *Chin. Phys.* B **20** 024208

[10] Hu Y T, Xiao X, Li Z Y, Li Y T, Fan Z C, Han W H, Yu Y D and Yu J Z 2011 *Chin. Phys.* B **20** 074208

[11] Huang J, Dong J R, Yang H, Zhang H Y, Tian C and Guo T Y 2011 *Chin. Phys.* B **20** 060702

[12] Xie H Q and Liu P K 2006 *Chin. Phys.* **15** 2042

[13] Peng W F, Hu Y L, Yang Z H, Li J Q, Lu Q R and Li B 2011 *Chin. Phys.* B **20** 028401

[14] Peng W F, Hu Y L, Yang Z H, Li J Q, Lu Q R and Li B 2011 *Chin. Phys.* B **20** 078401

[15] Kory C L, Dayton J A, Mearini G T, Malta D, Lueck M, Gilchrist K and Vancil B 2009 *Proc. IEEE Int. Vac. Electron. Conf.*, April 28–30, 2009, Rome, Italy p. 125

[16] Booske J H 2002 *Proc. IEEE Int. Vac. Electron. Conf.*, April 23–25, 2002, Monterey, USA p. 11

[17] Sengele S, Jiang H R, Booske J H, Kory C L, Weide D W V and Ives R L 2009 *IEEE Trans. Electron Dev.* **56** 730

[18] Fu C F, Wei Y Y, Duan Z Y, Wang W X and Gong Y B 2009 *Chin. Phys.* B **18** 2749

[19] Fu C F, Wei Y Y, Duan Z Y, Wang W X and Gong Y B 2008 *IEEE Trans. Electron Dev.* **55** 3582

[20] CST MWS Tutorials, CST Corp. [online] available: http://www.cst-china.cn/

[21] CST PS Tutorials, CST Corp. [online] available: http://www.cst-china.cn/

[22] Kory C L, Read M E, Ives R L, Booske J H and Borchard P 2009 *IEEE Trans. Electron Dev.* **56** 713

[23] Chao Z and Stevens G C 2006 *Proc. IEEE CEIDP*, October 15–18, 2006. Lamsas. ISA p. 19

[24] Cai J, Feng J J, Wu X P, Hu Y F, Qu B, Huang M G and Ma S Y 2007 *Proc. IEEE Int. Vacuum Electron. Conf.*, May 15–17, 2007, Kitakyushu, Japan p. 1

[25] Baig A, Wang J X, Barnett L R, Luhmann N J and Shin Y M 2011 *Proc. IEEE Int. Vac. Electron. Conf.*, February 21–24, 2011, Bangalore, India p. 351